steag
AST elektronik
A MEMBER OF STEAG GROUP

The 195th Meeting of
The Electrochemical Society, Inc

Seattle, WA; May 2-6, 1999

SYMPOSIUM
Advances in Rapid Thermal Processing

Chairs: F. Roozeboom, J. C. Gelpey, M. C. Ozturk, J. Nakos

INFLUENCE OF THERMAL NITRIDATION ON THE DIFFUSION OF ARSENIC DURING RAPID THERMAL ANNNEALING

W. Lerch[1], N. A. Stolwijk[2], S. D. Marcus[3], D. F. Downey[4], M. Schäfer[5]
[1] STEAG AST Elektronik GmbH, Dornstadt, Germany
[2] Institut für Metallforschung, Westfälische Wilhelms-Universität Münster, Germany
[3] STEAG AST Elektronik, Tempe (AZ), USA
[4] Varian Ion Implant Systems, Gloucester (MA), USA,
[5]CADwalk, Almendingen, Germany

Proceedings published as Volume 99-1 of the Electrochemical Society Proceedings Series

INFLUENCE OF THERMAL NITRIDATION ON THE DIFFUSION OF ARSENIC DURING RAPID THERMAL ANNNEALING

W. Lerch[1], N. A. Stolwijk[2], S. D. Marcus[3], D. F. Downey[4], M. Schäfer[5]
[1] STEAG AST Elektronik GmbH, Dornstadt, Germany
[2] Institut für Metallforschung, Westfälische Wilhelms-Universität Münster, Germany
[3] STEAG AST Elektronik, Tempe (AZ), USA
[4] Varian Ion Implant Systems, Gloucester (MA), USA,
[5]CADwalk, Almendingen, Germany

Nitridation of bare silicon surfaces in an ammonia-containing ambient is known to introduce vacancies in silicon at much lower temperatures than in a pure nitrogen ambient. The assumed vacancy excess during direct nitridation may enhance the diffusion of arsenic in silicon. After ultra-shallow implantation of As^+ with an energy of 1 keV to a dose of $\Phi \approx 1 \cdot 10^{15}$ cm^{-2} the change of the junction depth due to rapid thermal annealing (RTA) in an argon ambient with a varying but controlled concentration of ammonia (1000 ppm up to 100 %) is studied. Isochronal 10 s anneals are performed at 1000°C, 1050°C and 1100°C. Additionally, isothermal anneals at 1000°C, 1050°C and 1100°C for various times are performed as well. Concentration-depth profiles, measured by secondary ion mass spectroscopy were simulated within the SSUPREM IV computer code allowing for arsenic diffusion via neutral and negatively charged vacancies and silicon self-interstitials. From these experiments the RTA process for the formation of ultra-shallow junctions with arsenic can be optimized and the diffusion broadening of these near-surface implantations under non-equilibrium conditions better understood.

INTRODUCTION

The continued downscaling of CMOS devices to the 0.1 μm gate length feature and the increasing circuit complexity involves several process improvements and additions. In the critical section of the device fabrication process long-time furnace annealing steps have gradually been replaced by rapid thermal annealing (RTA) processes (1).

One of the main difficulties is the formation of low-resistance silicide contacts for the source and drain junctions of these small geometry devices while simultaneously maintaining low leakage currents and good transistor turn-off performance. This challenges junction annealing for controlling diffusion while fully activating the dopant. The formation of shallow n-junction using As implantation involves less problems than that of shallow p-junctions formed by boron or BF_2, both concerning ion-implant channeling (in particular boron) and diffusion broadening (2).

Previous publications (3), (4) of the present authors address the effect of RTA ambient oxygen on the diffusion of ultra-shallow $^{75}As^+$, $^{11}B^+$ and $^{49}BF_2^+$ implants. These works have shown a direct correlation between oxygen concentration and enhanced diffusion for B and

BF_2. We have also proposed a model based on the supersaturation of silicon self-interstitials caused by surface oxidation and on the kick-out diffusion model (3).

In a similar way the present work attempts to explain and model the diffusion characteristics of ultra-shallow 1 keV $^{75}As^+$ implants at a dose of $1 \cdot 10^{15}$ cm^{-2} as a function of ambient conditions. Since As diffusion in contrast to B diffusion is dominated by the vacancy mechanism, oxidizing ambients have little effect on the broadening of implanted profiles (4). Nitridizing ambients, however, may introduce vacancies in the bulk. Therefore we have annealed our implants for 10 s at 1000°C, 1050°C and 1100°C in argon ambients containing ammonia concentrations varying from 0~1 ppm to 100 %. Simulations of the resulting secondary ion mass spectroscopy (SIMS) profiles using the SSUPREM IV computer code, implemented in the desktop framework Athena (5), (6), reveal not only a direct nitridation-induced enhancement of As diffusion but also more indirect effects which appear to be due to capping of the silicon surface.

EXPERIMENTAL

For the experiments p-type, 200 mm Wacker prime Si wafers, (100)-orientation, 10-20 Ωcm, were used either for ion implantation or to monitor the silicon-oxynitride thickness growth during annealing independent of damage enhanced growth effects (7).

The arsenic implants (1 keV, $1.0 \cdot 10^{15}$ cm^{-2}) were performed on a Varian VIISion-80 PLUS low-energy high-current implanter at a tilt and twist angle of 0°. The beam current densities have been measured using an in-situ 2D beam profiler. A key issue for these ultra-shallow implantations of 210 Å depth (@ $1.0 \cdot 10^{18}$ cm^{-3}) is the variability of the native oxide. To avoid any influence prior to the implantation process a 30 s wet-chemical etch was performed in a HF (49 %):H_2O (1:40) solution. After implantation for each ammonia concentration a set of two wafers (a bare and an implanted wafer) were annealed in a STEAG AST Elektronik AST2800ε rapid thermal processing system (RTP). The recipes consist of a prolonged purge step for stabilization of the gas ambient, a prestabilization at 650°C, 10 s, followed by a final 10 s isochronal anneal at 1000°C, 1050°C and 1100°C, respectively. The ramp up rate to the soak time as well as the ramp down rate are 50 K/s. An average post-anneal uniformity (1σ) of less than 2 % on a 200 mm wafer was found for these ultra-shallow junctions.

The ammonia concentrations during the annealing step in Ar have been varied in a range of 0~1 ppm to 100 % within this work. Argon was used as inert carrier gas for avoiding unintentional and uncontrolled nitridation of silicon by nitrogen at higher temperatures (8). For the purpose of these experiments a low-flow ammonia mass flow controller (20 sccm/200 sccm) in conjunction with a standard (30 slm) argon mass flow controller were used to ensure the correct ammonia concentration.

The silicon-oxynitride thickness growth within the annealing time of 10 s was measured using a Plasmos SD3200 single wavelength ($\lambda = 633$ nm) ellipsometer (refractive index $n = 2.01$) with a relative measurement accuracy of 1 Å and a repeatability of 0.1 Å. Subsequent to ellipsometric characterization the sheet resistance was probed through the silicon-oxynitride on a KLA-Tencor RS100.

The implanted profiles have been analyzed using SIMS. The depth profiling was performed at Evans East Inc. using a Physical Electronics Φ 6600 SIMS spectrometer. The near-surface concentration accuracy has intentionally been improved by the use of an O-leak technique. The penetration depth for the SIMS measurements throughout this

publication is defined as the depth where the total concentration, sum of electrically and non-electrically active As atoms falls to a level of $3.0 \cdot 10^{18}$ cm^{-3}.

RESULTS AND DISCUSSION

Characterization of nitridation

The gaseous ambient during RTA plays a crucial role for the formation of ultra-shallow junctions because it may change the Si point defect equilibrium. For boron the injection of Si self-interstitials due to surface oxidation leads to an oxidation enhanced diffusion (OED) (3).

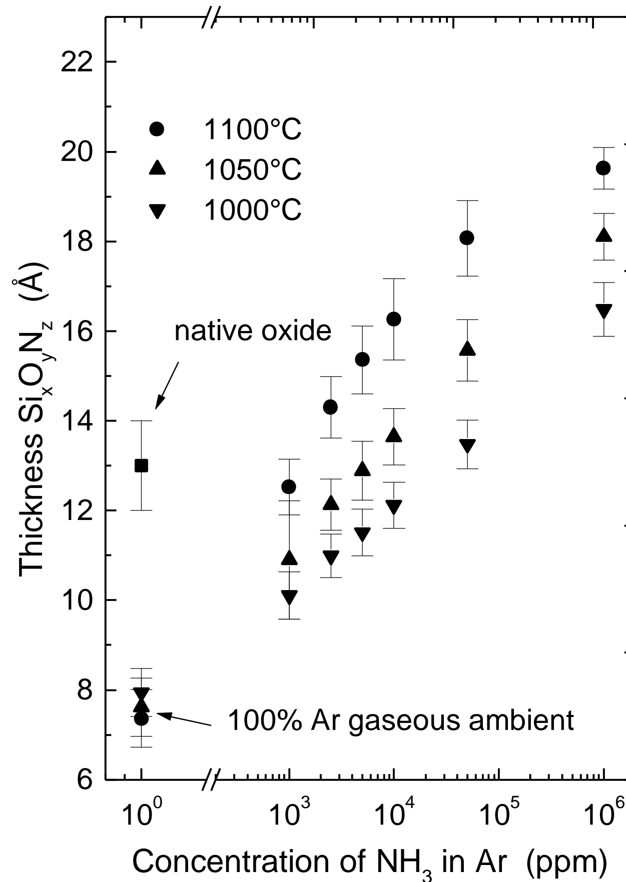

Figure 1: Silicon-oxynitride ($Si_xO_yN_z$) thickness versus relative ammonia concentration for various temperatures after isochronal annealing (10 s) of bare Si wafers. The refractive index used for the native oxide was $n = 1.465$, for all other measurements $n = 2.01$ of Si_3N_4 was used

Similar experiments were performed with arsenic ($^{75}As^+$, 2 keV, $1 \cdot 10^{15}$ cm^{-2}) (4). At 1050°C the junction depth was not much affected by the variation of the O_2 concentrations between 0~1 ppm (505 Å) and 50000 ppm (540 Å). The sheet resistance was almost constant. So, there was no pronounced OED effect; rather an oxidation retarded diffusion was observed. From the literature is known that the contribution of self-interstitials to arsenic diffusion is equal or less than 30 % (9). As a consequence, for the tailoring of as-

implanted arsenic profiles during the RTA we have to use, apart from the thermal budget (10), thermal nitridation since it has been established that this process injects vacancies into the bulk (11).

Jacob et al. (8) report that RTA annealing in N_2 at 1200°C to 1250°C resulted in an introduction of vacancies. However, annealings at and below 1100°C in pure nitrogen even for prolonged times did not result in measurable vacancy concentrations. Therefore the presented experiments were conducted in an ambient of NH_3 (reactive gas) and Ar (inert gas).

In Fig. 1 the dependence of the silicon-oxynitride thickness on the relative NH_3 concentration is displayed for bare silicon wafers which were annealed for 10 s at 1000°C, 1050°C and 1100°C. A monotonic increase of the silicon-oxynitride thickness with the NH_3 concentration is visible. However, the small thickness observed for 100 % Ar ambient (0~1 ppm NH_3) compared to the width of the native oxide layer reveals the effect of thermal etching.

Profile analysis

It is important to note that the prestabilization anneal at 650°C for 10 s did not change the as-implanted profile. In Fig. 2 an as-implanted profile together with an annealed one is displayed. The gaseous ambient was 100 % NH_3.

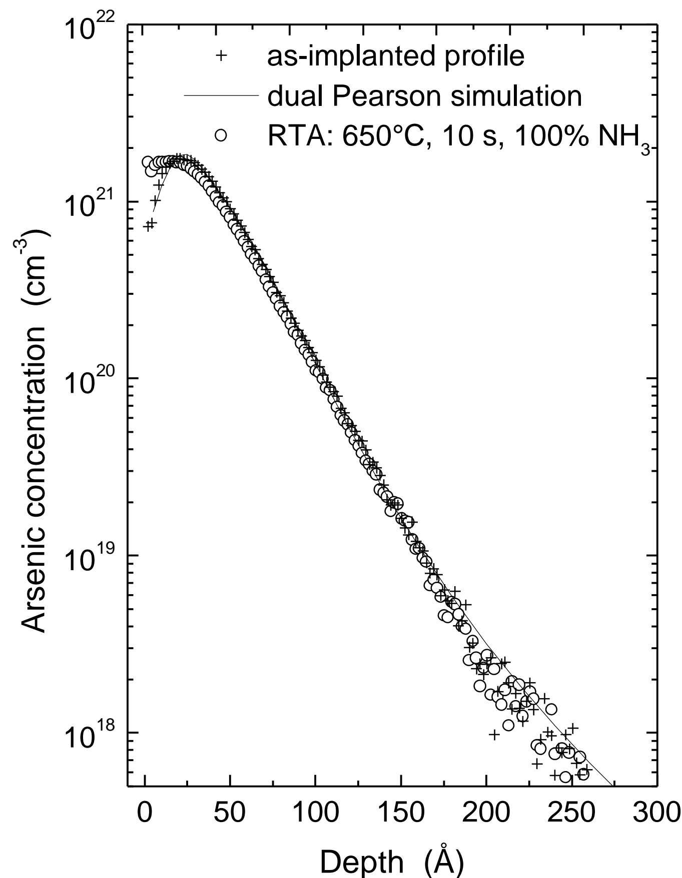

Figure 2: SIMS profile comparison of the As distribution after implantation to that after additional annealing (1 keV, $^{75}As^{+}$, $1 \cdot 10^{15}$ cm^{-2})

Even for this most reactive ambient there is no significant broadening of the profile after this low temperature process. Both implanted and annealed profiles are well described by a dual Pearson distribution.

In Fig. 3 As concentration depth profiles measured by SIMS after 1100°C diffusion / activation annealing are displayed together with the numerically simulated profiles. It is obvious, that the penetration depth increases monotonically i. e. (ignoring the nominally inert case) from 734 Å to 884 Å with NH_3 concentration running from 1000 ppm to 50000 ppm. Similar results were obtained for 1000°C and 1050°C. The shallowest penetration under nitridizing ambient at 1000°C is observed for 1000 ppm NH_3 and characterized by a depth of 354 Å. The corresponding depth at 1050°C is 492 Å.

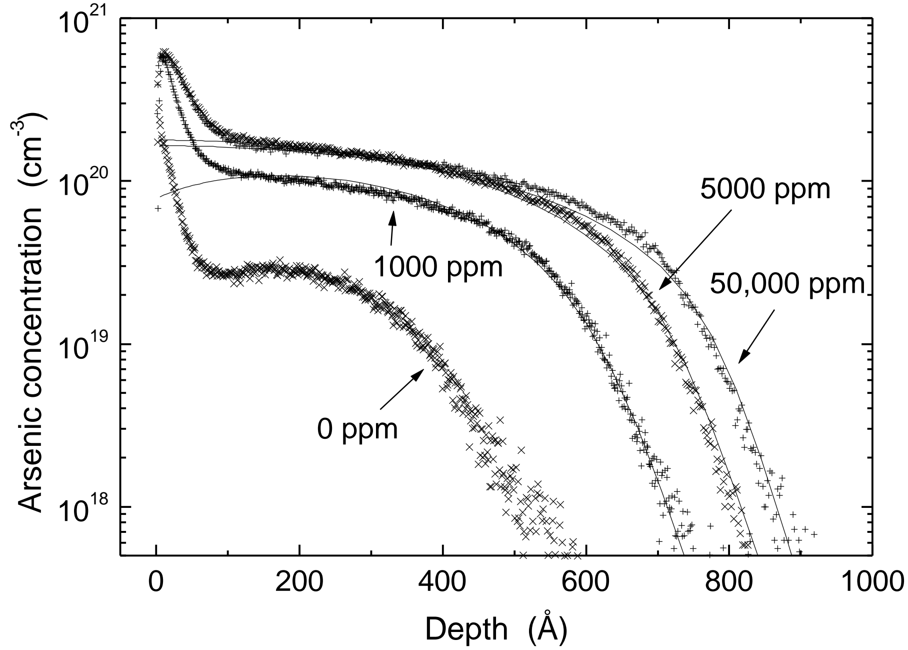

Figure 3: Arsenic SIMS profiles (x, +) after annealing for 10s at 1100°C for various concentrations of ammonia. The computer-simulated solid lines for nitridizing ambients show excellent agreement with the experimental data

Modeling of the As profiles was performed with the SSUPREM IV software package taking the as-implanted distribution (Fig. 2) as starting profile. For arsenic the local actual diffusivity D is given by

$$D = h\left(D_i^0 + D_i^-\left(\frac{n}{n_i}\right)\right) \qquad [1]$$

where D_i^0 denotes the As diffusivity via neutral point defects, i.e. Si vacancies (V^0) and Si self-interstitials (I^0), D_i^- the As diffusivity via singly negatively charged point defects (V^-, I^-), n the electron concentration which may exceed the intrinsic carrier density at the diffusion temperature $n_i(T)$, and h the electric-field enhancement factor which may approach the value 2 for high As concentrations. In the computer simulations all surface

reactions with ambient gases were switched off so that vacancies and self-interstitials were maintained at their thermal equilibrium values. Only a possible outflux of arsenic atoms through the Si surface was taken into account via the surface transport coefficient $\boldsymbol{n}_{surf}$ (TRANS parameter in SSUPREM IV). The pile-up of As observed in the region up to 100 Å beneath the Si surface is most probably due to segregation to the Si/Si-oxynitride interface. For arsenic as well as phosphorous and antimony this is described in the literature. Segregation coefficients of approximately 10 are usually quoted (12). This pile-up is not taken into consideration in the simulations.

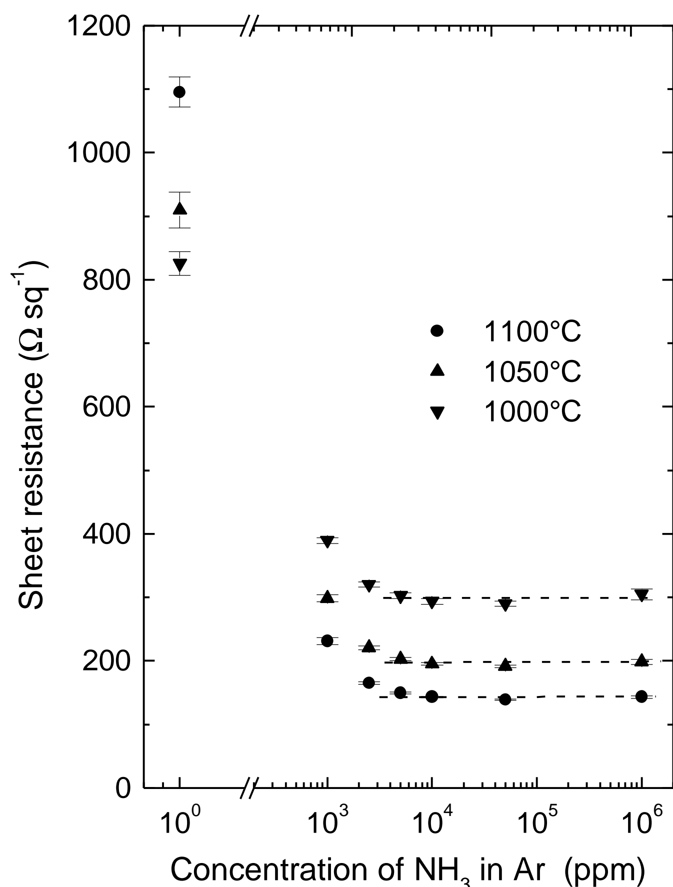

Figure 4: Sheet resistance versus ambient ammonia concentration as measured for the present As implants (1 keV, $1 \cdot 10^{15}$ cm^{-2}) annealed for 10 s at the indicated temperatures. The dashed lines represent saturation values

As illustrated in Fig. 3 for the 1100°C profiles, good or even excellent fits were obtained by optimizing D_i^0, D_i^- and $\boldsymbol{n}_{surf}$ being the only free parameters in the simulations. Moreover, the adjusted values of D_i^0 and D_i^- turned out to be constant within narrow error limits in the concentration range of 5000 ppm to 100 % of ammonia in Ar. In contrast, $\boldsymbol{n}_{surf}$ is orders of magnitude larger for 0~1 ppm NH_3 (100 % Ar) than for high NH_3 ambient concentrations. This reflects the substantial loss of As from the substrate for the lower NH_3 ambient concentrations as seen in Fig. 3, and hardly any loss for 100 % NH_3.

The same phenomenon is also apparent in Fig. 4, i. e. from the monotonic decrease of the sheet resistance with increasing NH_3 concentration which saturates at about 5000 ppm. The high sheet resistance for 0~1 ppm NH_3 is not only caused by extreme As loss but also by surface erosion due to thermal etching. Obviously, these unwanted effects make it difficult to obtain a satisfactory fit to the 0~1 ppm SIMS profile in Fig. 3.

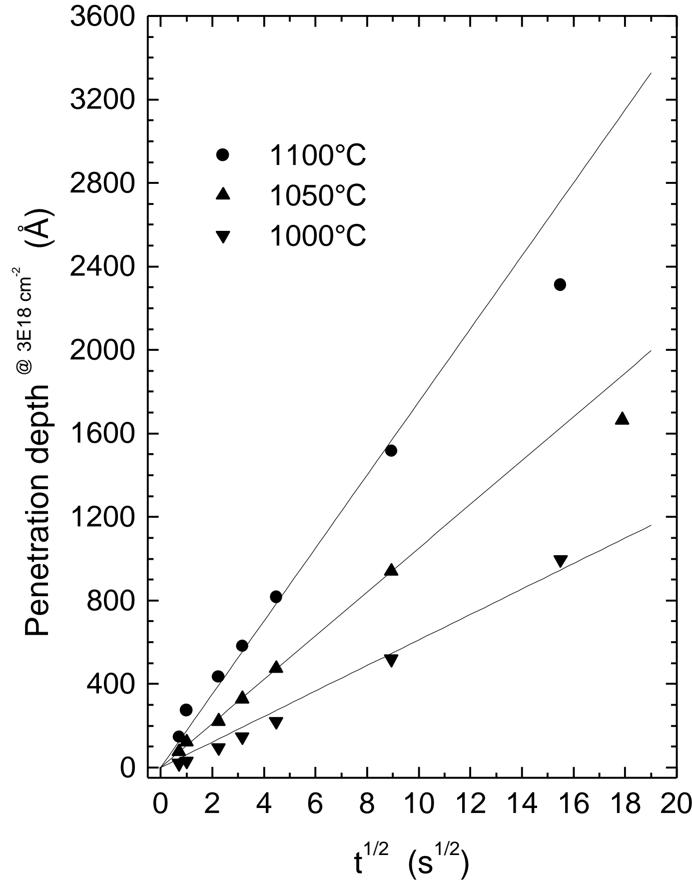

Figure 5: Penetration depth at $3\cdot10^{18}$ cm^{-3}, x_P, versus $\sqrt{t}$ after annealing for various times at three temperatures in 100 % NH_3 gaseous ambient. The solid lines represent theoretical predictions for a timely constant effective diffusivity

These findings imply that the increase of the As penetration depth with increasing NH_3 concentration shown in Fig. 3 is *not* caused by a *direct* nitridation-enhanced diffusion effect as resulting from vacancy injection. Rather the present results can be rationalized by a more *indirect* surface capping effect which correlates with the growing thickness of the $Si_xO_yN_z$ layer exhibited by Fig. 1. Concomitantly, the ever better prevention of As loss from the substrate leads to an increase of the As concentration in the plateau region beneath the surface. In turn, these increased concentrations give rise to higher electron densities and therefore to a stronger self-doping enhancement of the diffusivity (see Eq. [1]). In Fig. 5 the netto penetration depth, x_P, at $3\cdot10^{18}$ cm^{-3} versus the annealing time is displayed for the anneals with 100 % ammonia. In x_P a correction is made for the penetration depth of the as-implanted profile. There is a fair linear dependence up to a time of 100 s. For longer times x_P tends to be shallower than the extrapolation of the linear fit.

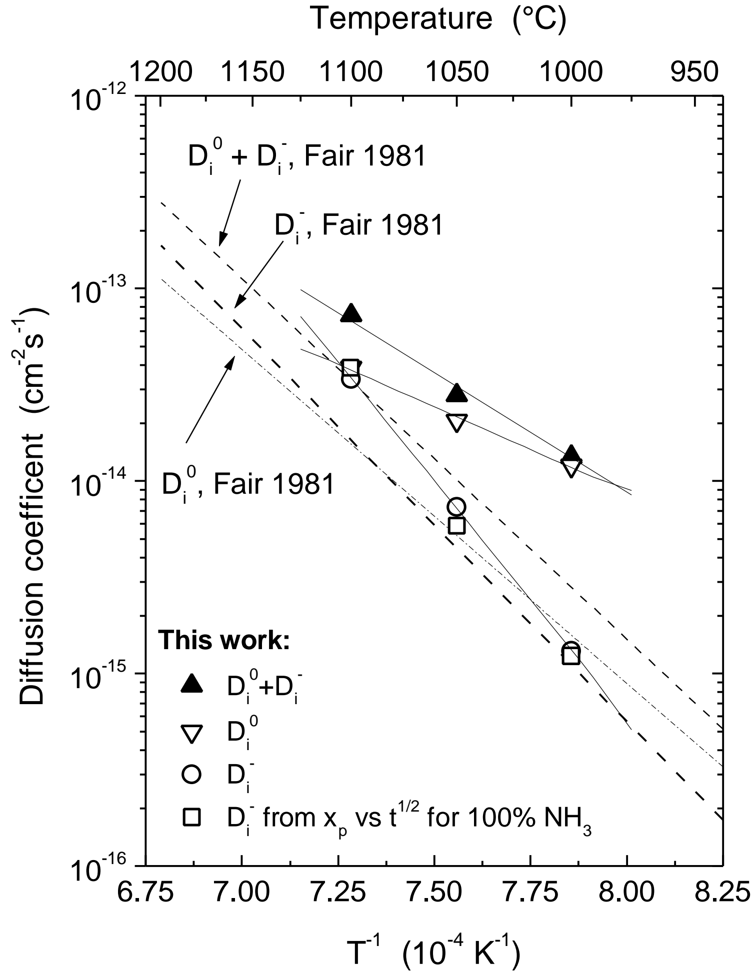

Figure 6: Intrinsic diffusion coefficients of As under NH_3 ambients, present work (symbols) compared to literature data for inert ambient diffusion (13) (dashed lines)

Diffusion coefficients

Fig. 6 reveals the intrinsic As diffusion coefficients that were obtained from computer modeling of the measured profiles, together with literature data (13). The present data are averages over NH_3 ambient concentrations from 5000 ppm to 100 % NH_3 for which no significant differences were observed. Not only the individual diffusivities D_i^0 and D_i^- are displayed in Fig. 6 but also their sum $D_i = D_i^0 + D_i^-$ which is the total As diffusivity under intrinsic conditions. Fig. 6 also includes D_i^- estimated from the time dependence of the penetration depth x_P shown in Fig. 5. This estimation is based on the relationship (see Eq. [1] with $h = 2$)

$$x_P \approx 2 \cdot \sqrt{D \cdot t} \approx 2 \cdot \sqrt{2 \cdot D_i^- \cdot \left(\frac{n}{n_i}\right) \cdot t} \qquad [2]$$

which approximately holds in high concentration regions $(D_i^-(n/n_i) >> D_i^0)$. It is seen that the two ways of calculating D_i^- lead to a reasonably good agreement for all temperatures.

Comparing the total intrinsic diffusivity $D_i^0 + D_i^-$ under NH_3 ambient (this work) with that for inert conditions (13) we see a diffusion enhancement of a factor of 3.5 at 1000°C and of nearly 2 at 1100°C. This picture does not change much if we take other established data for intrinsic As diffusion from the literature (14), (15). Enhancements of similar magnitude have been found in earlier As diffusion experiments carried out in NH_3 ambient at 1100°C (9). This lends credit to the view that we are dealing in the present study with nitridation-enhanced diffusion.

However, some caution seems appropriate since residual implantation damage usually gives rise to strong transient enhanced diffusion (TED) effects in the case of B and P in Si. For As, several studies report pertinent TED effects (e.g.(16), (17)), whereas others explicitly state the absence of TED (e.g. (18), (19)). Downey and Jones (20) state that during the implantation of 1 keV $^{75}As^+$ at a dose of $1{\cdot}10^{15}$ cm^{-2} no extended defects or trapped interstitials are formed and that the amorphous layer is about 120 Å thick. Therefore, for the present implantation followed by recovery annealing at 650°C the TED effect is likely to be of minor importance. This conclusion is supported by the observation that x_P versus $\sqrt{t}$ holds for annealing times in the range 0-100 s.

CONCLUSIONS

Annealing of implanted $^{75}As^+$ (1 keV, $1{\cdot}10^{15}$ cm^{-2}) was performed in an RTP system for various times and temperatures under different concentrations of ammonia in argon. The nitridation of the surface leads to capping of the surface which influences the retained dose of the implanted ion and therefore indirectly enhances As penetration via an increased self-doping effect. Nevertheless from the simulation of the SIMS profiles under various ammonia concentrations also a direct nitridation-induced enhancement, probably due to vacancy injection, was found from the comparison with inert ambient diffusivities (13), (14), (15). Both influences on As diffusion are almost constant for ammonia concentrations in argon varying from 5000 ppm to 100 %. From the processing efficiency point of view 5000 ppm of ammonia seems to be an optimal choice.

ACKNOWLEDGMENTS

The authors would like to thank Dr. G. Roters for helpful discussions and critical reading of the manuscript. We are indebted to Dr. Z. Nenyei, the Applications Lab staff of STEAG AST Elektronik GmbH, the VARIAN IIS team, and co-authors of our previous publications.

REFERENCES

(1) F. Roozeboom in Advances in Rapid Thermal and Integrated Processing, edited by F. Roozeboom, NATO ASI Series E, Vol. 318, (Kluwer 1996)

(2) D. F. Downey, S. L. Darayanani, M. Meloni, K. Brown, S. B. Felch, B. S. Lee, S. D. Marcus, J. C. Gelpey, *Mat. Res. Soc. Symp. Proc.* **470**, 299 (1997)

(3) W. Lerch, M. Glück, N. A. Stolwijk, H. Walk, M. Schäfer, S. D. Marcus, D. F. Downey, J. W. Chow, H. Marquardt, *Mat. Res. Soc. Symp. Proc.* **525** 237 (1998)

(4) D. F. Downey, J. W. Chow, W. Lerch, J. Nieß, S. D. Marcus, *Mat. Res. Soc. Symp. Proc.* **525** 263(1998)

(5) Computer code SSUPREM IV developed at the Integrated Circuits Laboratory Stanford University by R. W. Dutton and J. D. Plummer

(6) ATHENA trademarked and commercially available process simulation framework developed by SILVACO International comprising SSUPREM IV

(7) J. F. Götzlich, K. Haberger, H. Ryssel, *Radiation Effects* **47** 203 (1980)

(8) M. Jacob, P. Pichler, H. Ryssel, R. Falster, M. Cornara, D.Gambaro, M. Olmo, M. Pagani, GADEST’97, Diffusion and Defect Data, Part B (*Solid State Phenomena*) Vols. 57-59 349 (1997)

(9) P. Fahey, G. Barbuscia, M. Moslehi, R. W. Dutton, *Appl. Phys. Lett.* **46**(8) 784 (1985)

(10) Z. Nenyei, C. Grunwald, W. Lerch, J. Nieß, D. F. Downey, R. Ostermeir, 6th International Conference on Advanced Thermal Processing of Semiconductors, RTP’98, Sep. 9-11, 1998; Kyoto, Jp

(11) P. M. Fahey, P. B. Griffin, J. D. Plummer, *Rev. Mod. Phys.* **61**(2) 289 (1989)

(12) S. M. Sze, VLSI Technology, 2nd Edition, (McGraw-Hill 1988), pp. 332-340

(13) R. B. Fair, in Impurity Doping, edited by F. F. Y. Wang (North Holland, Amsterdam) p. 315 (1981)

(14) D. A. Antoniadis, A. M. Lin, R. W. Dutton, *Appl. Phys. Lett.* **33** 1030 (1978)

(15) C. Hill, *Proc. Electrochem. Soc.* **81-5** 988 (1981)

(16) Y. Kim, H. Z. Massoud, R. B. Fair, *J. Electron. Mater* **18** 143 (1989)

(17) R. B. Fair, *J. Electrochem. Soc.* **137** 667 (1990)

(18) T. O. Sedgwick, T. O., A. E. Michel, S. A. Cohen, V. R. Deline, G. S. Oehrlein, *Appl. Phys. Lett.* **47** 949 (1985)

(19) H. Park and M. E. Law, *Appl. Phys. Lett.* **58** 733 (1991)

(20) D. F. Downey and K. S. Jones, presented at the 12th International Conference on Ion Implantation Technology, June 22-26, 1998, Kyoto Jp